



Cite this: DOI: 10.1039/d3ee04363k

# All-in-one hybrid atmospheric water harvesting for all-day water production by natural sunlight and radiative cooling†

Jiaxing Xu,<sup>a</sup> Xiangyan Huo,<sup>a</sup> Taisen Yan,<sup>a</sup> Pengfei Wang,<sup>a</sup> Zhaoyuan Bai,<sup>a</sup> Jingwei Chao,<sup>a</sup> Ronggui Yang,<sup>\*c</sup> Ruzhu Wang<sup>id</sup> <sup>\*ab</sup> and Tingxian Li<sup>id</sup> <sup>\*ab</sup>

Extracting water from air is a promising method to solve the global challenge of water scarcity. Sorption-based atmospheric water harvesting (S-AWH) has the capability of all-weather water production from air under arid or humid climates. However, high energy consumption and low water production are two long-standing bottlenecks to realizing efficient S-AWH. Herein, we propose a low-carbon sustainable strategy for atmospheric water generation by synergistically harvesting heat from natural sunlight for water desorption and cold from the universe for water condensation. The synergistic effects of transmittance-type radiative cooling membranes enable the hybrid AWH to realize efficient S-AWH by lowering water condensation temperature in the daytime and providing extra water production in the nighttime. Notably, the hybrid AWH device exhibits water productivity of up to 3654 g m<sup>-2</sup> day<sup>-1</sup>. This work offers an energy-efficient method for all-day atmospheric water generation by synergistically harvesting energy from sunlight and sky radiative cooling.

Received 15th December 2023,  
Accepted 2nd April 2024

DOI: 10.1039/d3ee04363k

rsc.li/ees

## Broader context

Water scarcity is becoming one of the most severe global challenges threatening the survival of humankind. Sorption-based atmospheric water harvesting has the potential to quench global thirst as it has the unique ability to extract water from dry air. Prior techniques were limited by low water generation efficiencies; one of the major reasons is the high condensation temperature impeding the release of captured water in sorbents. Here, we report a radiative-cooling-enhanced strategy to achieve sub-ambient temperature condensation. Integrating enhanced sorption-based water harvesting and extra dew water collection at night, the daily water productivity significantly increases to over 3.6 L m<sup>-2</sup>. This work paves the way towards energy-efficient atmospheric water harvesting based on synergistically utilizing solar heating and radiative cooling.

## Introduction

Freshwater shortage is one of the most severe global challenges threatening social and economic development.<sup>1</sup> Water scarcity is particularly acute in arid regions, which are generally landlocked and lack natural liquid water resources.<sup>2</sup> To quench the thirst of people living in arid regions, exploiting new water sources becomes highly valuable. The amount of water in the

atmosphere is as much as ~13 000 billion tons, six times more than the water in all the rivers on earth,<sup>3</sup> denoting that the atmospheric water source is sufficient and sustainable.<sup>4,5</sup> Sorption-based atmospheric water harvesting (S-AWH) has attracted much attention in recent years due to its ability to be driven by solar energy and being feasible anytime and anywhere.<sup>6,7</sup> Through the great efforts of materials scientists, various novel sorbents have been proposed as potential candidates for sorption-based AWH with extraordinary working performance and advantages, including MOFs,<sup>8–11</sup> hydrogels,<sup>12–15</sup> and composite sorbents.<sup>16–20</sup> Substantial efficient attempts to improve the working performance of sorption-based AWH devices were also reported,<sup>21–25</sup> however, a gap exists between proof-of-concept and practical applications due to the low energy utilization efficiency of S-AWH devices.<sup>26</sup> Thus, it is urgent to make comprehensive technology innovations on both materials and devices, accelerating the development and application of AWH technologies.

<sup>a</sup> Institute of Refrigeration and Cryogenics, School of Mechanical Engineering, Shanghai Jiao Tong University, Shanghai 200240, China. E-mail: litx@sjtu.edu.cn, rzwang@sjtu.edu.cn

<sup>b</sup> Research Center of Solar Power & Refrigeration, Shanghai Jiao Tong University, Shanghai 200240, China

<sup>c</sup> School of Energy and Power Engineering, Huazhong University of Science and Technology, Wuhan 430074, China. E-mail: ronggui@hust.edu.cn

† Electronic supplementary information (ESI) available. See DOI: <https://doi.org/10.1039/d3ee04363k>

Low energy efficiency is a long-standing bottleneck for realizing energy-efficient S-AWH, and it can be attributed to the high energy consumption used for water desorption by heating the sorbent and used for water condensation by cooling the condenser. The former has attracted much attention in recent years and it can be well mitigated by designing low-enthalpy sorbents<sup>27</sup> and efficient solar collectors.<sup>28</sup> However, little attention has been focused on the condenser design, and it is still a great challenge to develop advanced condensers with lightweight, small volume, and low energy consumption for efficient water condensation. In particular, the condensation temperature has a significant influence on the water productivity of S-AWH. The temperature difference between water desorption and water condensation is one of the essential prerequisites for driving water release and condensation in S-AWH devices. Therefore, exploiting energy-efficient condensation strategies is highly valuable to improving energy efficiency and water productivity.

Ambient air is widely regarded as the cold source for water condensation in many reported AWH devices, but scaled-up S-AWH devices need a large heat exchange surface or forced air convection to reduce the heat-exchange temperature difference, such as employing heat-pipe-type heat sinks and air-fan-assisted metal-fin condensers.<sup>9,22</sup> Our previous work revealed that the condenser temperature will be as high as 16.5 °C above ambient if water is fast condensed on a finned radiator without an active heat dissipation strategy.<sup>29</sup> Significantly, the hot ambient temperatures in arid regions result in a high condenser temperature, corresponding to a high dew point, hampering the water desorption–condensation or even causing a failure in water collection.<sup>10</sup> Therefore, although natural air convection cooling is an energy-efficient way to dissipate heat, its low heat exchange coefficient of  $\sim 10 \text{ W m}^{-2} \text{ K}^{-1}$  is insufficient to cover all condensation heat.<sup>30</sup>

To lower the condensation temperature, active cooling technologies such as thermoelectric coolers<sup>8</sup> and compression-type chillers<sup>23</sup> are efficient heat dissipation strategies, providing a lower condensation temperature than ambient but consuming extra electricity. Compared with electricity-powered cooling technologies, zero-energy sky radiative cooling with a low carbon footprint is a promising technology to harvest cold from the universe,<sup>31</sup> potentially providing a sub-ambient temperature. Nighttime radiative cooling technology has been used for building energy saving and water harvesting for a long time.<sup>32</sup> In nature, the darkling beetles in the Namib desert use nighttime radiative cooling to collect dew water from the air.<sup>33</sup> Recently, a continuous dew-based AWH (D-AWH) strategy was reported using radiative cooling both in the daytime and nighttime,<sup>34</sup> and the water productivity was up to  $50 \text{ g m}^{-2} \text{ h}^{-1}$ .<sup>35</sup>

Integrating radiative cooling with S-AWH has attracted attention for promoting water harvesting from the air. Kim *et al.* first reported the potential of nighttime radiative cooling to lower the temperature of sorbents, allowing the sorbents with mild water affinity to work under low RH conditions.<sup>9</sup> Recently, Wang *et al.*<sup>36</sup> and Zhu *et al.*<sup>37</sup> developed

multifunctional sorbents with extraordinary water harvesting capacity, high stability, and radiative cooling functions. The nighttime radiative cooling enabled a low sorption temperature to facilitate the exothermic water harvesting process.<sup>38</sup> Our recent work also demonstrates that nighttime radiative cooling can be employed to cool the sorbent and generate electricity simultaneously.<sup>39</sup> However, daytime radiative cooling is rarely reported for promoting water condensation in S-AWH systems.

Herein, a hybrid atmospheric water harvesting strategy is proposed to realize energy-efficient AWH by introducing all-day radiative cooling technology. Instead of using radiative cooling to assist atmospheric water harvesting by cooling the sorbent, we propose a novel approach that leverages daytime radiative cooling to lower the water condensation temperature of the S-AWH device, thereby enhancing the water release from the sorbent and water condensation during the daytime. Moreover, we also exploit nighttime radiative cooling to either cool the sorbent or achieve direct dew-based atmospheric water harvesting, depending on the relative humidity of the ambient air. Outdoor all-day water harvesting experimental results demonstrate that daytime radiative cooling enables a sub-ambient temperature for fast water condensation with a maximum temperature drop of 5.1 °C and extra collected water at night if the nighttime RH is higher than 70%. Benefiting from the synergistically coupling S-AWH with D-AWH, the AWH device delivers a high daily water productivity of  $3654 \text{ g m}^{-2}$  driven by only sunlight and radiative cooling.

## Results and discussion

### Concept design on all-day hybrid atmospheric water harvesting

We propose a low-carbon and sustainable strategy, synergistically harvesting energy from natural sunlight and the cold universe, for driving energy-efficient and all-day hybrid water production from the air. We rationally design an all-in-one hybrid AWH device by integrating sorption-based AWH (S-AWH) and radiative cooling-driven dew-based AWH (D-AWH) (Fig. 1A). The S-AWH operates by heating the sorbent material with sunlight, which causes it to release water vapor into the closed chamber. The elevated dew point in the chamber induces the condensation of water vapor on the radiative cooling surface at the top, realizing water production. The daytime radiative cooling from the cold universe is used to accelerate the water collection of S-AWH by lowering the condenser temperature. In contrast, the D-AWH relies on the nighttime radiative cooling effect, and the device is opened and exposes to ambient moisture, which enables the direct condensation of ambient moisture on the radiative cooling surface. Simultaneously, the sorbents capture water from the air at night, replenishing the water in the sorbents for S-AWH function the next day.

AWH technologies are designed for applications in arid climates, where the RH is low during the day.<sup>40</sup> However, arid regions typically exhibit large diurnal variations in temperature and humidity, which enable direct dew water condensation at

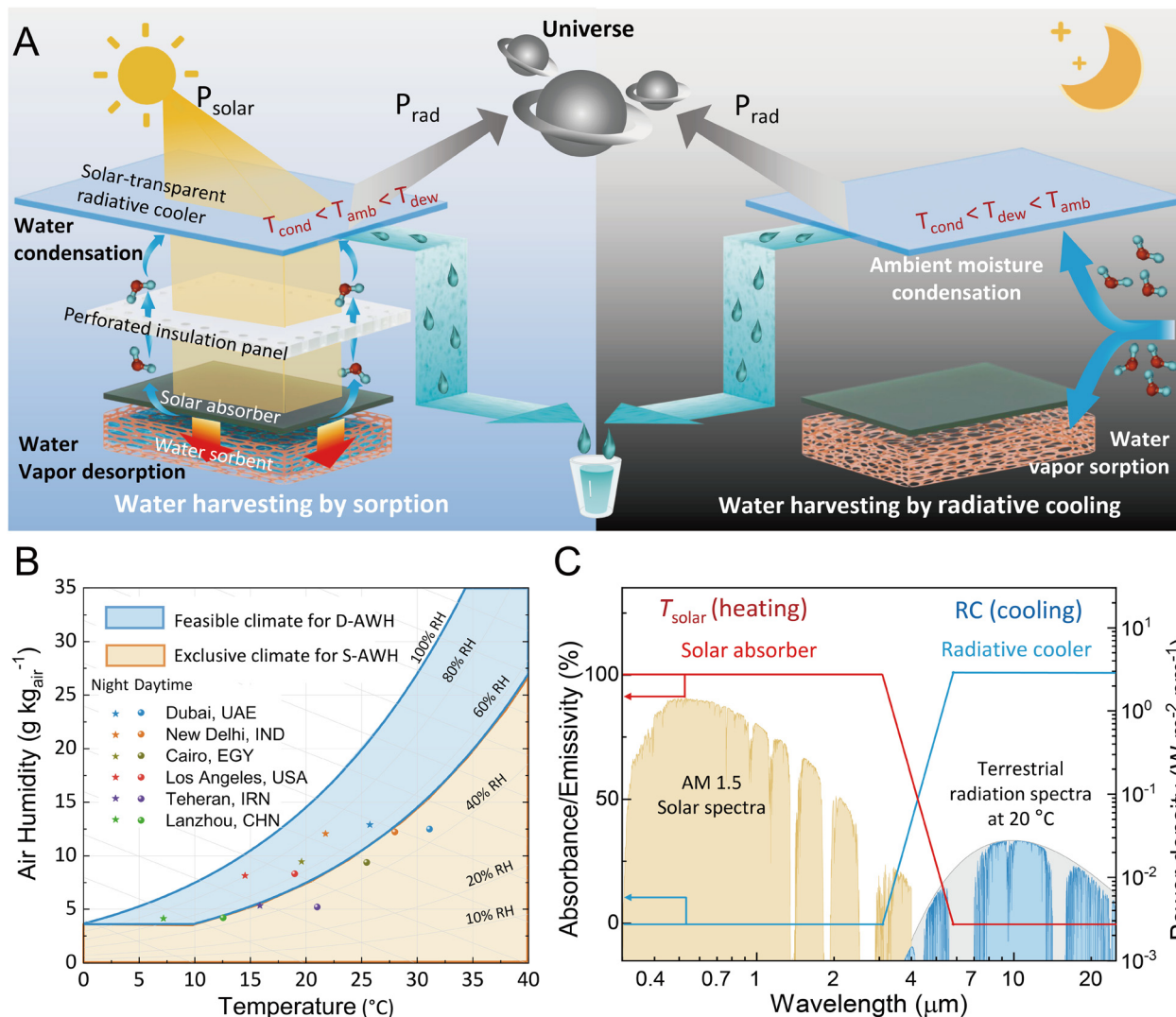


**Fig. 1** All-day hybrid atmospheric water harvesting (AWH) by integrating S-AWH in daytime and D-AWH in nighttime. (A) Working principle of all-day hybrid AWH. A transmittance-type radiative cooling (TRC) membrane enables the working feasibility of radiative heating from natural sunlight for water desorption and radiative cooling from the cold universe for water condensation simultaneously. The S-AWH occurs in daytime (left diagram), in which sunlight passes through the TRC membrane heating the sorbent to release water vapor, the released water condenses on the surface of TRC membrane by daytime radiative cooling. The D-AWH occurs in nighttime (right diagram), in which the sorbent captures water vapor from the air for the water replenishment; meanwhile, water vapor in the ambient moisture condenses on the TRC membrane to directly produce water at night. (B) A psychrometric chart showing the average climate conditions of typical cities located in arid or semi-arid regions. The average temperatures and RH are separately marked to show the operating adaptability of the all-in-one hybrid AWH strategy with sorption-based AWH in daytime and radiative cooling-driven D-AWH in the nighttime. The symbol of stars represents the average annual maximum daytime temperature, and the symbol of spheres represents the average annual minimum nighttime temperature. Data come from Meteornorm.<sup>41</sup> (C) The ideal spectral profile of a TRC membrane and solar absorber for achieving all-day hybrid AWH.

night (see Fig. S1 for climate data, ESI<sup>†</sup>). In cases where the nighttime RH is insufficient for direct dew water collection, the sorbent can be cooled by nighttime radiative cooling to achieve a higher water sorption capacity.<sup>9</sup> This method will be tested and discussed in the last section. The hybrid water production strategy utilizes the temperature/RH variations between daytime and nighttime to realize S-AWH and D-AWH, and the feasible climate conditions for D-AWH can be further enlarged with the development of radiative cooling technology (Fig. 1B).

To realize a hybrid AWH, the transmittance-type radiative cooling (TRC) membrane and solar collector need exceptional spectral characteristics (Fig. 1C): (i) high solar transparency and low solar absorbance for the TRC membrane at wavelengths ranging from 0.2  $\mu\text{m}$  to  $\sim 3 \mu\text{m}$ ; (ii) high emissivity for the TRC membranes at the infrared spectral region ranging from  $\sim 4 \mu\text{m}$  to 25  $\mu\text{m}$ . While selective emitters with high emissivity at the atmospheric window (8  $\mu\text{m}$  to 13  $\mu\text{m}$ ) have been widely used to achieve lower cooling temperatures, we demonstrate that emitters with high emissivity over a broad infrared

spectrum can provide higher cooling power for water condensation, as most water-harvesting systems operate at or above ambient air temperature where the water condensation is a strong exothermic process;<sup>34,42</sup> (iii) high solar absorptivity for the solar collector at the wavelength ranging from 0.2  $\mu\text{m}$  to  $\sim 3 \mu\text{m}$ ; (iv) low emissivity for the solar collector at the infrared spectral region ranging from  $\sim 4 \mu\text{m}$  to 25  $\mu\text{m}$ . To achieve the hybrid AWH, we select commercial polydimethylsiloxane (PDMS) as a TRC membrane and commercial selective solar absorber panel (cermet-coated aluminum) as a sunlight-to-heat collector. By coupling the TRC and selective solar absorber in the same one occupied physical area, the compact all-in-one AWH device not only realizes high energy-efficiency solar heating but also provides extra cooling power from the cold universe for accelerating the water condensation of S-AWH in the daytime and driving the dew water condensation of D-AWH at night.

### Thermal design and energy analysis of the all-in-one hybrid AWH

Although many novel sorbents have emerged in recent years, their water harvesting capacities generally cannot be totally exploited in practical AWH devices due to the incomplete water release during the thermo-driven water desorption–condensation process. Here, we define a critical parameter, desorption relative humidity ( $\text{RH}_{\text{dc}}$ ), to index the capacity of water release depth at the thermo-driven water desorption stage, as expressed by the following equation,

$$\text{RH}_{\text{dc}} = \frac{P_{\text{vap}}}{P_{\text{sat}}(T_{\text{dc}})} \quad (1)$$

where  $P_{\text{vapor}}$  and  $P_{\text{sat}}(T_{\text{de}})$  represent the water vapor pressures inside the chamber (near the sorbent) and the saturated water vapor pressure at desorption temperature ( $T_{\text{de}}$ ). The water productivity ( $\omega_{\text{S-AWH}}$ ) of the S-AWH device can be estimated by calculation of the equilibrium water sorption capacity ( $\omega_{\text{sorb}}$ ) minus the residual water inside sorbents ( $\omega_{\text{de}}$ ) under desorption conditions, expressed as the equation,

$$\omega_{\text{S-AWH}} = \omega_{\text{sorb}}(\text{RH}_{\text{sorb}}) - \omega_{\text{de}}(\text{RH}_{\text{de}}) \quad (2)$$

where values of  $\omega_{\text{sorb}}$  and  $\omega_{\text{de}}$  can be found in the isothermal water sorption and desorption curves of the water sorbent at specific  $\text{RH}_{\text{sorb}}$  and  $\text{RH}_{\text{de}}$ , respectively. Therefore, to improve the AWH capacity, reducing the residual water at the desorption stage is as important as increasing the water uptake at the sorption stage, pursuing  $\text{RH}_{\text{de}}$  as low as possible. If we ignore the condensation resistance, the condensation temperature is equal to the dew point temperature, and the vapor pressure near the sorbent ( $P_{\text{vapor}}$ ) can be expressed by the condensation temperature and vapor transfer pressure difference between sorbent and condenser ( $\Delta P$ ), as  $P_{\text{vapor}} = P_{\text{sat}}(T_{\text{cond}}) + \Delta P$ . Since the  $\Delta P$  highly depends on the structures and sizes of devices, we ignore this parameter for a simplified calculation. Using the Magnus's form equations,<sup>43</sup> the desorption relative humidity can be expressed by only

desorption temperature and condensation temperature as in eqn (3).

$$\text{RH}_{\text{dc}} = \frac{P_{\text{sat}}(T_{\text{cond}})}{P_{\text{sat}}(T_{\text{de}})} = \frac{\exp\left(\frac{17.27T_{\text{cond}}}{237.3 + T_{\text{cond}}}\right)}{\exp\left(\frac{17.27T_{\text{de}}}{237.3 + T_{\text{de}}}\right)} \quad (3)$$

Accordingly, water condensation temperature strongly influences the working capacity of S-AWH. More information can be found in the ESI† Note S1.

For salt-based composite sorbents, water sorption/desorption shows multi-step processes, *viz*: water absorption/evaporation ( $\omega_{\text{ab}}$ ), deliquescence/crystallization of salt hydrates ( $\omega_{\text{deli}}$ ), and chemical sorption/decomposition ( $\omega_{\text{chem}}$ ) (Fig. 2A).<sup>19</sup> However, the multi-step water release process is hardly completed under natural sunlight if the desorption temperature is insufficient or the condenser temperature is too high. Specifically, the crystallization and chemical desorption will not occur during the water release process if the RH of desorption is higher than the deliquescence/crystallization RH (DRH) and chemical sorption/desorption RH (CRH) (Fig. 2B).

Furthermore, we demonstrate the influence of condensation temperature on the single-cycle S-AWH productivity of pure LiCl and pure CaCl<sub>2</sub>, at the consumption of sorption at 30 °C, 1.2 kPa and desorption at 8 °C, 4.2 kPa, based on eqn (3) (Fig. 2C). Accordingly, a low condensation temperature near or below ambient temperature is desirable to enable thorough release of captured water from the sorbent. More information about the S-AWH capacities of pure salts at different condensation temperatures is given in the ESI† Note S1 and Fig. S2 and S3.

To experimentally assess the impact of condensation temperature on enhancing water productivity, we chose our previously reported salt composite, LiCl@rGO-SA, as the working material in this study, which has a high water sorption capacity (Fig. 2D).<sup>29</sup> The AWH capacity can be theoretically enhanced 2–3 times by lowering the condenser temperature (Fig. 2E), and the dynamic water release tests of LiCl@rGO-SA are in good agreement with water sorption–desorption equilibrium characteristics (Fig. 2F).

Although salt-based composite sorbents are more sensitive to the condensation temperature due to the multistep sorption–desorption mechanism, a low water condensation temperature is also desirable for classical physical sorbents (such as zeolites, silica gels) and MOFs to utilize low-grade thermal energy for S-AWH by reducing the water desorption temperature (see Fig. S4, ESI†),<sup>48–52</sup> especially for the sorbents with slowly rising water isotherm characters. Therefore, advanced thermal design is essential to improve S-AWH capacity by lowering the condenser temperature for water collection.

For conventional solar-driven S-AWH devices with passive air-cooling, thermal analysis shows that more than half of the input solar energy cannot be utilized for AWH due to the heat loss through thermal radiation and convection, and significant heat loss causes a low energy efficiency ( $\sim 16\%$ ) (see the ESI†

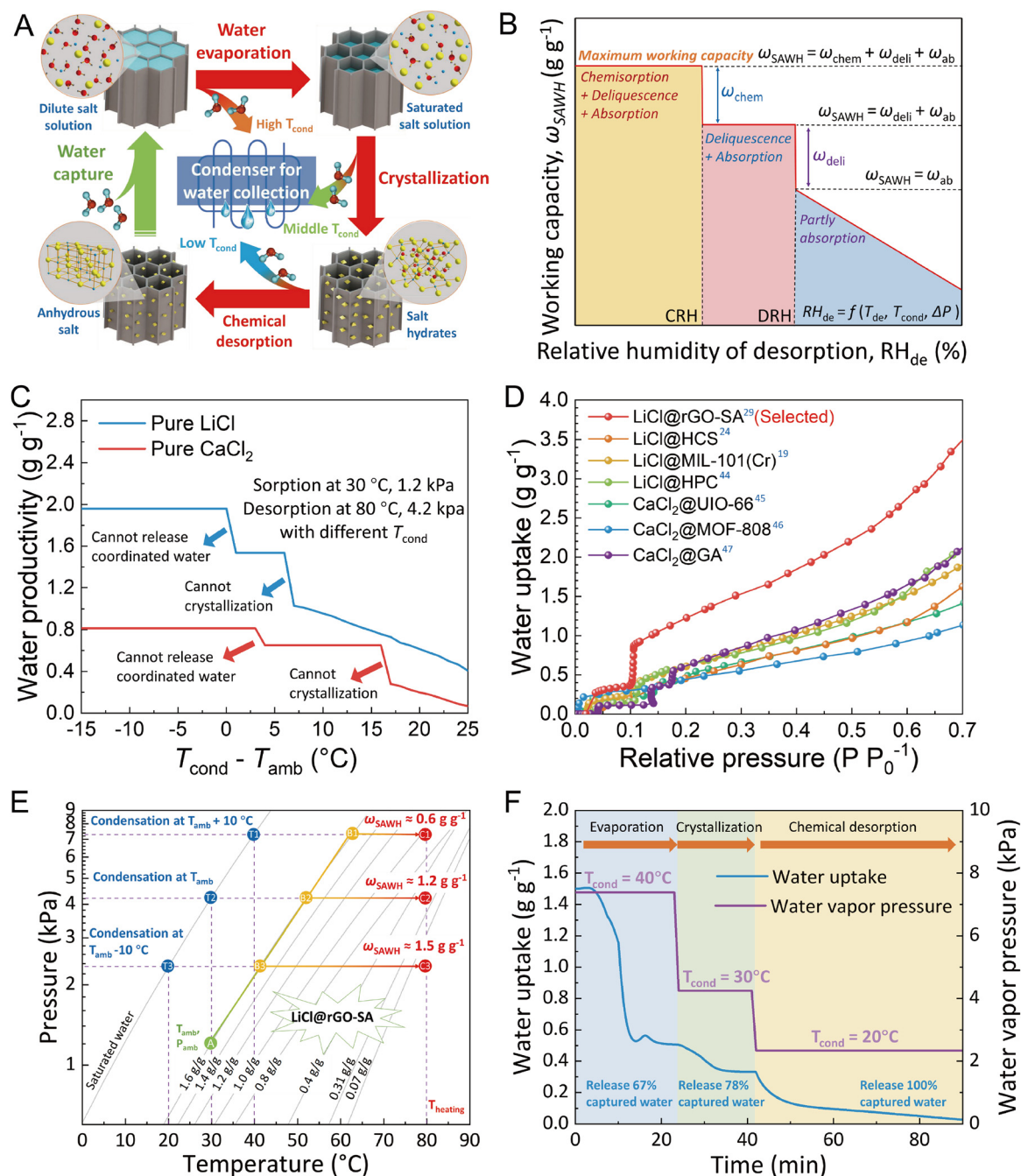


**Fig. 2** Understanding the influence of condensation temperature on sorption-based AWH. (A) Schematic showing multi-step water release processes of composite sorbents, viz: water evaporation ( $\omega_{ab}$ ), crystallization ( $\omega_{deli}$ ), and chemical decomposition ( $\omega_{chem}$ ). (B) Working capacity of S-AWH under different desorption  $RH_{de}$ , determined by water condensation temperature ( $T_{cond}$ ). (C) Theoretical S-AWH working capacity of pure LiCl and pure CaCl<sub>2</sub>, working at 30 °C, 1.2 kPa for sorption, 80 °C, 4.2 kPa for desorption, and varying condensation temperatures for water collection. (D) Water sorption isotherms of recently reported state-of-the-art salt-based composite sorbents.<sup>19,24,29,44–47</sup> (E) Working capacity of S-AWH using LiCl@rGO-SA at different condensation temperatures for a given heating temperature. (F) The influence of condensation temperature on the multi-step water desorption of LiCl@rGO-SA at a constant desorption temperature of 80 °C under different water vapor pressures of 7.4 kPa, 4.2 kPa, and 2.3 kPa, corresponding to the condensation temperatures at 40 °C, 30 °C, and 20 °C, respectively.

Note S2 and Fig. S5). Moreover, a bulky air-cooling condenser is indispensable for conventional S-AWH devices to realize a low condensation temperature. To address the drawbacks, we develop a new thermal design for the hybrid AWH device by employing radiative cooling to lower the condensation

temperature and insulation panel to suppress heat loss (Fig. 3A). We first develop a thermal network model to analyze and optimize the thermal design of AWH devices (see the ESI† Note S3 and Fig. S6–S8). The net cooling power by the radiative cooler (PDMS membrane) is expressed as,

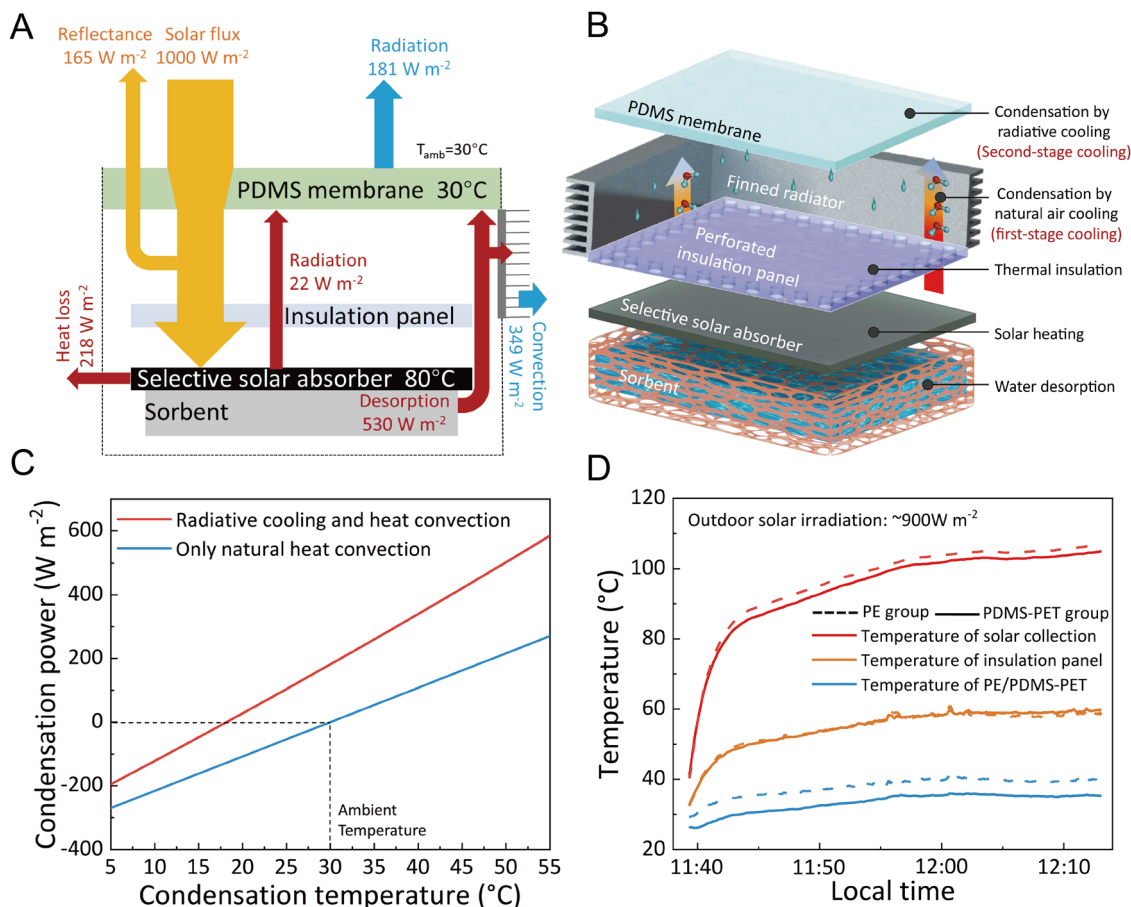


**Fig. 3** Theoretical analysis and thermal design of all-in-one hybrid AWH assisted by radiative cooling. (A) Energy flux of a hybrid AWH device with a radiative-cooling PDMS membrane at a solar heating temperature of 80 °C. (B) Schematic showing a cascade condensing strategy using air-cooling and radiative-cooling condensers for hybrid AWH. The tandem design strategy allows the finned condenser to cover the major sensible heat of hot vapor and PDMS to realize a low condensation temperature. (C) Cooling power by radiative cooling-convective heat (red line) and by only natural heat convection (blue line) at different condensation temperatures. (D) Temperature profiles of selective solar absorber, insulation panel, and TRC membrane under outdoor experiments without sorbents. The dotted lines are the temperatures of the PE group, and the solid lines are the temperatures of the PDMS-PET group.

$$P_{\text{net,cond}} = P_{\text{rad,PDMS}} - P_{\text{atm}} - \alpha_{\text{PDMS}}P_{\text{solar}} - \alpha_{\text{water}}P_{\text{solar}} - P_{\text{net,rad,ab}} - P_{\text{nonrad}} \quad (4)$$

where  $\alpha_{\text{PDMS}}$  and  $\alpha_{\text{water}}$  are the solar absorbances of PDMS and condensed water, respectively. To obtain an effective net cooling power ( $P_{\text{net,cond}}$ ) by radiative cooling, the heat absorption must be suppressed, including radiation heat from the atmosphere, solar absorption by PDMS ( $\alpha_{\text{PDMS}}P_{\text{solar}}$ ) and condensed water ( $\alpha_{\text{water}}P_{\text{solar}}$ ), radiative heat from solar absorber ( $P_{\text{net,rad,ab}}$ ), and the non-radiative heat transfer by convection ( $P_{\text{nonrad}}$ ). We measured the absorbance of pure water and analyzed the solar absorbance of water film at different thicknesses (see Fig. S9, ESI<sup>†</sup>), and found that the condensed water on the PDMS surface needs to be removed in a timely manner or diffused as a thin film to decrease solar absorption. To solve the scattering effect of sunlight on water droplets on the hydrophobic surface of PDMS, commercial super hydrophilic poly(ethylene terephthalate) (PET) is covered on the bottom surface of PDMS to form a combined PDMS-PET membrane,

making its water contact angle decrease from 110.2° to 11.3°, together with an apparent weakened light scatter effect (see Fig. S9, ESI<sup>†</sup>), ensuring the stability of continuous radiative cooling power output during the water condensation process.

Thermal analysis shows that the TRC membrane can provide net cooling power by optimizing the thickness of the water film and employing hydrophilic PET, but its net cooling power is very low ( $\sim 7.9 \text{ W m}^{-2}$ ). The poor net cooling power is caused by the heat input from the atmosphere ( $164.6 \text{ W m}^{-2}$ ) and hot solar absorber ( $109.0 \text{ W m}^{-2}$ ) at the bottom of the AWH device (see the ESI<sup>†</sup> Note S3). Thus, we introduce a perforated insulation panel between the TRC membrane and solar absorber to suppress convective heat input from the solar absorber (Fig. 3B), whose radiative heat transfer is negligible, ascribing to its selective solar absorbance characters (see Fig. S7, ESI<sup>†</sup>). The cooling power can be enhanced up to  $181 \text{ W m}^{-2}$  at a typical condensation temperature of 30 °C if these heat inputs are well eliminated (Fig. 3C), always higher than air-cooling due to PDMS radiative cooling effects. However, the

radiative-cooling power is insufficient to cover all condensation heat of water vapor ( $\sim 530 \text{ W m}^{-2}$ ) unless the condensation temperature is above  $50 \text{ }^\circ\text{C}$  (Fig. 3C) or the PDMS surface area is enlarged by 2.93 times. Therefore, we here propose a cascade heat dissipation strategy for accelerating water condensation by installing the air-cooling aluminum heat exchanger without active cooling and radiative-cooling PDMS membrane in series as two condensers (Fig. 3B), where the released hot water vapor is first cooled down by the former (first-stage cooling), and then further cooled by PDMS to perform water condensation on the surface of the PET membrane (second-stage cooling), enabling a low condensation temperature through the cascade cooling strategy. Although sky radiative cooling cannot cover all of the condensation heat in the current stage, its advantages of being lightweight, small in volume, energy-efficient, and having a lower cooling temperature than natural air cooling make it a potential alternative to partially replace the traditional condenser for realizing more efficient and compact S-AWH (Table S1, ESI<sup>†</sup>).

To verify the effect of radiative cooling on lowering the condenser temperature of hybrid AWH in the daytime, we design two all-in-one AWH devices, one with a PDMS-PET TRC membrane that has radiative cooling effects, and the other with polyethylene (PE) membranes without radiative cooling (only air cooling) (see Fig. S10–S12, ESI<sup>†</sup>). We set a fair comparison control experiment by replacing the TRC membrane with a PE film, named the PE group, while other components of the AWH device remained identical. To eliminate the solar absorption of the device, we coat the commercial specular reflective membrane on the surface of the aluminum and acrylic shell of the device (see Fig. S10, ESI<sup>†</sup>). We compare the temperature evolutions of two AWH devices without sorbents under indoor one sun irradiation ( $1000 \text{ W m}^{-2}$ ) and outdoor natural sun irradiation ( $\sim 900 \text{ W m}^{-2}$ ). Neither of the devices undergo radiative cooling during the indoor experiments, while only the device with PDMS-PET undergoes radiative cooling during the outdoor experiments (see Fig. S13, ESI<sup>†</sup>). The outdoor experimental results show that the PDMS-PET always has a lower temperature than PE due to the radiative cooling effect (Fig. 3D). The large temperature drop ( $\sim 5 \text{ }^\circ\text{C}$ ) confirms that a high cooling power is realized by introducing TRC even without a convective cover. Compared with typical reflection-type daytime radiative coolers, the transmittance-type daytime radiative cooler has a simpler structure, effective cooling power, and allows solar heating in the same physical area (see the ESI<sup>†</sup> Note S4 and Table S1).

### Demonstration of the all-in-one hybrid AWH device for all-day water production

Based on the thermal analysis, we design an all-in-one hybrid AWH device with a layer-by-layer compact structure (Fig. 4A) and evaluate its condensation efficiency using air-cooling and radiative-cooling methods. Our latest developed salt-based composite sorbents,<sup>29</sup> LiCl@rGO-SA with vertically aligned pore structures, are used to demonstrate the feasibility of the all-day hybrid AWH device for water harvesting

from the air due to the high water uptake and multi-step sorption isotherm character (see Fig. 2D). To achieve high water production per unit area during one sorption-desorption cycle, we prepared the composite sorbent with a higher thickness (10 mm), and it remains the satisfactory thermal conduction ability (see Fig. S13, ESI<sup>†</sup>). All the sorbents capture water at  $30 \text{ }^\circ\text{C}$ , 50% RH overnight in a constant temperature and humidity chamber before the outdoor tests. To evaluate the contribution of the TRC membrane, we carried out outdoor experiments on the roof of our Green Energy Lab (GEL) in Shanghai, China (see Fig. S14A, ESI<sup>†</sup>), and performed comparative tests of two all-in-one hybrid AWH devices with and without a TRC membrane (Fig. 4B). We find the AWH device with TRC has a lower temperature than ambient (see Fig. S15, ESI<sup>†</sup>), confirming that TRC is effective for lowering the condenser temperature. In addition, the sorbents inside two AWH devices have almost similar temperature profiles under natural sunlight (see Fig. S14B, ESI<sup>†</sup>), indicating that the TRC membrane has a negligible impact on solar heating for sorbents.

A remarkable difference between the two devices during water condensation processes (see Movie S1, ESI<sup>†</sup>) verifies that radiative cooling can accelerate water collection by lowering water vapor pressure and condensation temperature under the S-AWH mode in the daytime. As a result, the proposed TRC-assisted S-AWH exhibits a high-water production of up to  $1072 \text{ g}_{\text{water}} \text{ m}^{-2} \text{ solar}$  and  $0.72 \text{ g}_{\text{water}} \text{ g}^{-1} \text{ sorbent}$  per cycle within three hours (Fig. 4C). The calculated S-AWH rate is as high as  $357.3 \text{ g m}^{-2} \text{ h}^{-1}$ , which is one of the highest rates among the reported passive sunlight-direct-driven S-AWH devices under similar working climates.<sup>8,9,22</sup> The higher AWH productivity in the view of both per gram of sorbent and per unit of solar collection area can be attributed to the improved sorption capacity of sorbents and the rational design of coupling solar heating and radiative cooling on the same occupied area, respectively. The TRC membrane provides a sub-ambient temperature for enhanced condensation due to the daytime radiative cooling by PDMS. The temperature of the TRC membrane gradually increases when water vapor begins to condense on its surface, but it always maintains a low temperature, particularly lower than ambient at the initial stage (Fig. 4D). Besides, the water condensation on both the TRC membrane and air-cooling aluminum radiator indicates the feasibility of the proposed cascade heat dissipation strategy for water condensation.

Although the absolute value of radiative cooling temperature,  $5.1 \text{ }^\circ\text{C}$  lower than the ambient temperature, is not high, we want to emphasize that traditional natural air-cooling AWH devices cannot realize a condensation temperature lower than the ambient temperature. In particular, we observe that the air-cooling aluminum condenser has a temperature up to  $7.5 \text{ }^\circ\text{C}$  higher than the ambient temperature (see Fig. S16, ESI<sup>†</sup>). These results confirm that the radiative cooling by PDMS-PET can provide a lower condensation temperature below the ambient temperature and considerable cooling power from the cold universe for accelerating the water condensation of S-AWH

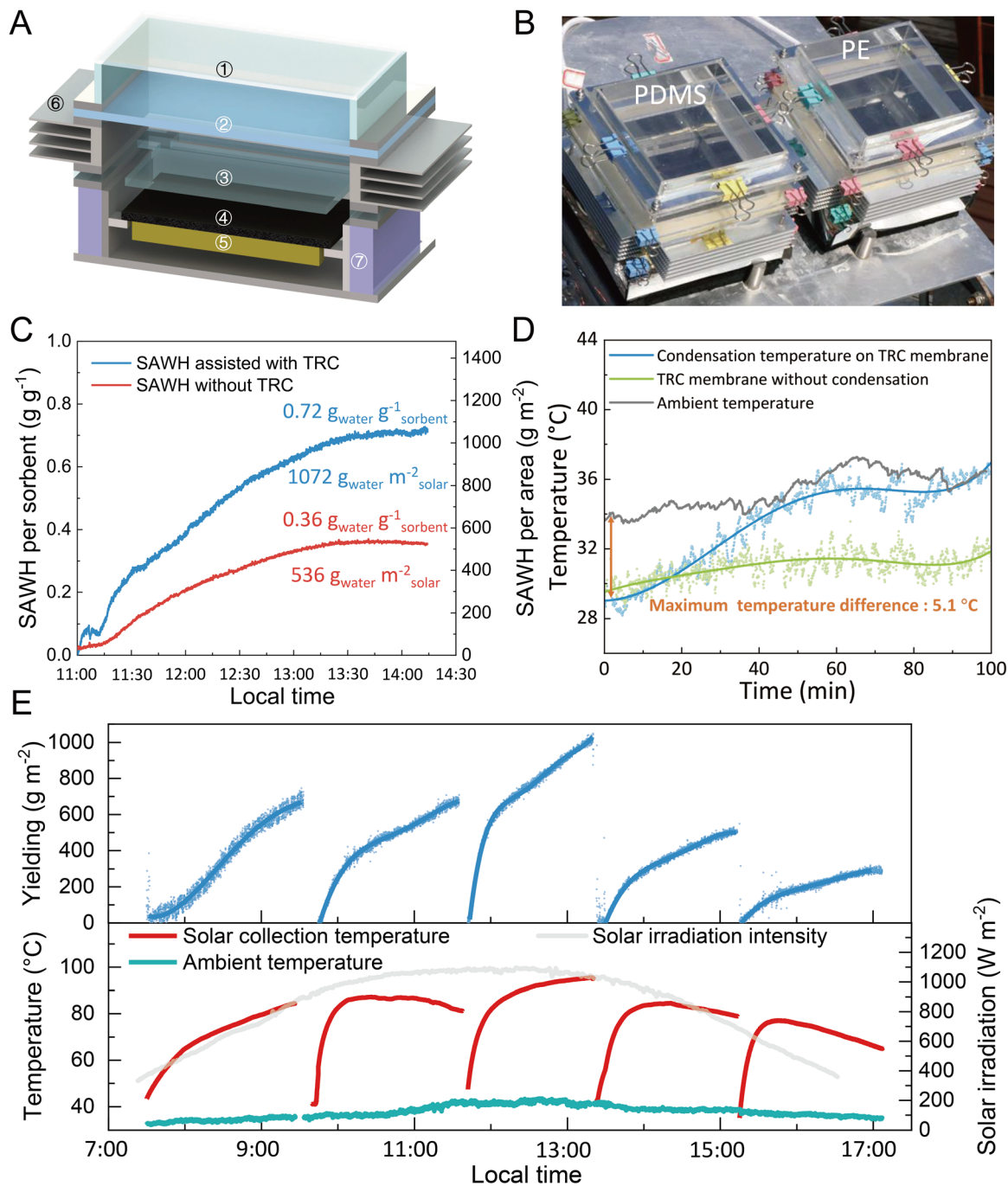


**Fig. 4** Outdoor demonstration of the all-in-one hybrid AWH device in the daytime. (A) Schematic showing the layer-by-layer structure of the all-in-one hybrid AWH device for all-day water production, mainly consisting of PE cover ①, sunlight-transparent PDMS-PET TRC membrane ②, perforated thermal insulation panel ③, selective solar absorber ④, water sorbent ⑤, aluminum finned heat sink ⑥, and thermal insulation enclosure ⑦. (B) Photograph of two sunlight-driven S-AWH devices, wherein the left one is covered with a TRC membrane and the right one is covered with a PE membrane. (C) S-AWH performance of two devices with and without a TRC membrane in view of both per unit sorbent and solar heating area, tested on May 1, 2021. (D) Temperature evolutions of the TRC membrane and ambient air during water collection in the daytime. (E) Experimental demonstration of the hybrid AWH device for multiple daytime water harvesting cycles on August 4, 2022, on the roof of our lab in Shanghai, China.

in the daytime. Specifically, the temperature drop by PDMS radiative cooling brings a lower water vapor pressure for water desorption in the S-AWH with TRC when compared to the S-AWH without TRC (see Fig. S17, ESI<sup>†</sup>); thus, promoting the

multi-step water desorption of sorbents during the water release-collection process (Fig. 2A). The S-AWH with TRC membrane releases 85.7% of the captured water while only 56.3% is released by sorbents in the S-AWH device without

TRC, indicating PDMS radiative cooling contributes to a 52.2% improvement in the water production of S-AWH.

To show all-day water productivity in a whole day, we carried out multiple S-AWH cycles during the daytime after water sorbents capture water from the air and reach sorption

saturation at night (see Fig. S18, ESI<sup>†</sup>). The water sorbents are packed vertically at night to capture water from the ambient air simultaneously, and then are manually transferred to the closed AWH chamber one by one in the daytime for water desorption using a batch-processed strategy.<sup>55</sup> In comparison

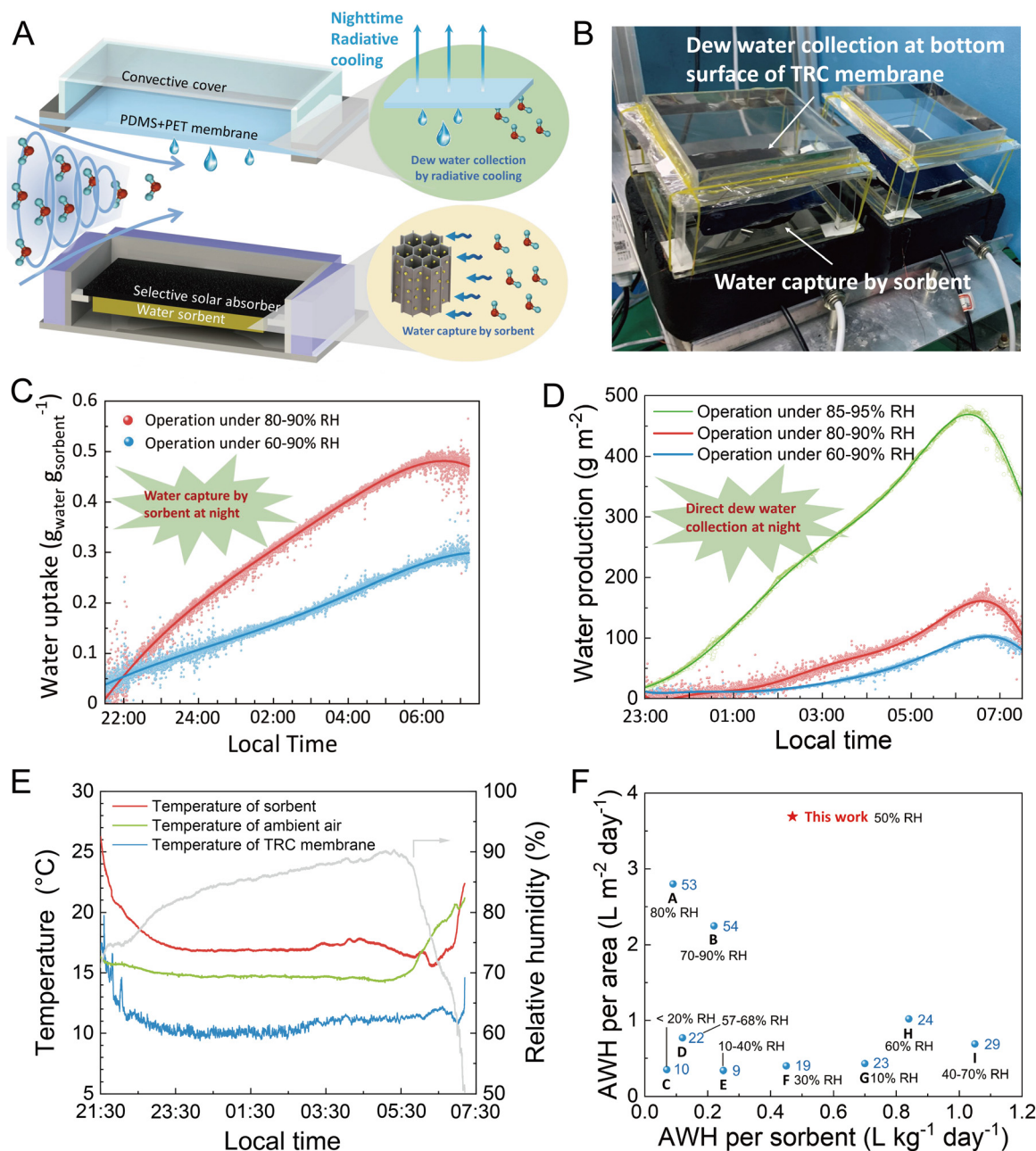


**Fig. 5** Outdoor demonstration of the all-in-one hybrid AWH device at nighttime. (A) Schematic showing the working principle of TRC-driven D-AWH and water vapor capture of S-AWH from air by sorbents in the nighttime. (B) A photo of the all-in-one hybrid AWH device in the open state on the roof of our green energy lab (GEL) at Shanghai Jiao Tong University (SJTU), Shanghai, China. (C) Water capture of  $\text{LiCl}@r\text{GO}-\text{SA}$  sorbents at night without other auxiliary facilities under two different ambient RH. (D) Outdoor water collection of D-AWH at night under different ambient air conditions, tested on May 1, June 6, and June 22 in 2021. (E) Temperature profiles of  $\text{LiCl}@r\text{GO}-\text{SA}$  sorbent, TRC membrane, and ambient air, together with the ambient air RH during the D-AWH demonstration on May 1, 2021. (F) The comparison of practical AWH performance between the proposed all-in-one AWH device and the recently reported solar-driven AWH devices in perspectives of both daily water productivity per kg of sorbent and per unit of area.<sup>9,10,19,22–24,29,53,54</sup> We performed the S-AWH and D-AWH tests on the same occupied physical area with five different sorbents. Thus, we calculated the areal water productivity based on the projected area of the device. The mass of all five pieces of sorbents was determined to calculate the water productivity per mass of sorbent.

with the rapid-cycling S-AWH employing only one piece of sorbent, the S-AWH based on a batch-process strategy uses several pieces of sorbents in favor of realizing higher water productivity per unit of area (see the details in Fig. S19, ESI†). The same physical area is used for continuously multi-times water desorption in the daytime, resulting in high water productivity per unit of projected area. In contrast, if we pursue a S-AWH device with a less mass of sorbent, a rapid-cycling strategy is more desirable. The duration of every water desorption–condensation process is controlled at two hours by tuning the thickness of LiCl@rGO-SA to 10 mm. Therefore, the device with five sorbents can perform five water desorption cycles in the daytime from 7:00 to 17:00 on Aug. 4, 2022, maximizing the utilization of daily solar energy. Summing up the collected water of the five pieces of water sorbents, the daytime S-AWH capacity reaches as high as 3182 g m<sup>-2</sup> (Fig. 4E).

During the nighttime, the all-in-one hybrid AWH device works at TRC-driven D-AWH mode and water capture of S-AWH from air concurrently (Fig. 5A). The AWH device is manually open to allow the moisture to diffuse in, and the perforated insulation panel is removed to reduce the heat and mass transfer resistance (Fig. 5B). When the temperature of the TRC membrane is lower than the dew-point of ambient air under radiative cooling, the ambient moisture will condense on the surface for realizing D-AWH. Simultaneously, the sorbents capture water from the air, realizing water backfill (Fig. 5C). The water vapor is only allowed to condense on the bottom surface of the TRC membrane in the AWH device to avoid the attenuation of the radiative-cooling effect caused by the condensed water droplets. The water uptake by sorbent for S-AWH ranges between 0.32–0.49 g g<sup>-1</sup><sub>sorbent</sub>, and the water collection by D-AWH reaches 102–472 g m<sup>-2</sup> (Fig. 5C and D) under different RH. We find the sorbent has a temperature about 3 °C higher than the ambient temperature due to the sorption heat released by LiCl@rGO-SA. In contrast, the TRC membrane always maintains a low temperature of about 5 °C lower than ambient air during nighttime due to the radiative cooling effects (Fig. 5E). The water production rate of D-AWH is as high as 11.3–52.4 g m<sup>-2</sup> h<sup>-1</sup> under different RH conditions (see Fig. S20, ESI†), which is comparable with the D-AWH data in the reported literature.<sup>34,35</sup>

Integrating the daytime S-AWH capacity of 3182 g m<sup>-2</sup> and nighttime D-AWH capacity of 472 g m<sup>-2</sup>, the hybrid AWH device realizes an impressive maximum all-day water production of 3654 g m<sup>-2</sup> day<sup>-1</sup>, corresponding to a high average water production rate of 152 g m<sup>-2</sup> hour<sup>-1</sup>. By integrating solar heating and radiative cooling in a single occupied area with a rational thermal design, and employing a batch-process working strategy, our all-in-one hybrid AWH device achieves the highest daily water productivity per unit of projected area among all reported sunlight-driven AWH devices (Fig. 5F). The proposed all-in-one hybrid AWH device shows a high thermal efficiency of 26.1% (see the ESI† Note S4 and Table S2). Considering the all-day AWH device is designed for the potential portable applications, we also provided the S-AWH

capacity in the view of the weight and space of the whole device (exclusive of sensors), whose values are 41.7 mL<sub>water</sub> kg<sub>device</sub><sup>-1</sup> day<sup>-1</sup> and 25.2 mL<sub>water</sub> L<sub>device</sub><sup>-1</sup> day<sup>-1</sup>. The truth of great gaps between water productivity per unit of sorbent and per unit of device proves once again that the research on AWH technology should not be limited to developing new sorbents, but also needs to focus on improving other components of the device, such as the heat collector, insulation, condenser and so on, for realizing energy-efficient, lightweight, and compact operation.

The fabrication cost of the all-in-one AWH device, excluding sensors, is estimated to be approximately 10.85 USD, as detailed in Table S3 (ESI†). Therefore, the initial investment cost of the all-day AWH device with a water productivity of 1 L day<sup>-1</sup> is calculated to be around 296.9 USD. In addition, we further use a levelized cost of water (LCOW) framework to evaluate the techno-economics of the all-day AWH device by incorporating the lifetime capital and operating expenditures over the lifetime water production,<sup>56</sup> whose value is 0.11 USD per liter of water (see details of the calculation in Table S4, ESI†).

To further verify the practical feasibility of all-day AWH in arid climates, we evaluated the water productivity of outdoor S-AWH and D-AWH in Kunming, Yunnan province, China (see the photos in Fig. S21, ESI†). We carried out five days of continuous S-AWH and D-AWH tests from Mar. 6, 2024, to Mar. 10, 2024. We successfully realized S-AWH and D-AWH on Mar. 7 with a total water productivity of 3126 g m<sup>-2</sup> (Fig. S22, ESI†). Moreover, the device steadily operated for five days with continuous S-AWH water productivities of 2392 g m<sup>-2</sup>, 2749 g m<sup>-2</sup>, 2216 g m<sup>-2</sup>, 2021 g m<sup>-2</sup>, and 2491 g m<sup>-2</sup>, respectively (Fig. S23, ESI†). However, we only realized D-AWH on the sunny day of Mar. 7 among these days, in which a clean sky without any clouds results in enough high diurnal temperature and RH differences (Fig. S24, ESI†), triggering direct water condensation on the radiative cooling membrane with a D-AWH water productivity of 377 g m<sup>-2</sup> at night.

Accordingly, it is worth pointing out that radiative cooling-driven D-AWH has the risk of no water production at low RH in arid regions, where the dew point of air may be too low to be reached by the current radiative cooling technologies. In the case of low RH, nighttime radiative cooling can promote the water sorption of sorbents by lowering the sorption temperature (see Fig. S25, ESI†). However, we want to mention that the extra water sorption in sorbents by nighttime radiative cooling requires extra heat consumption to drive the water desorption in the daytime. As a result, nighttime radiative cooling can improve the water sorption of sorbents, but it cannot enhance the energy efficiency. Hence, to improve AWH with the fully exploited sky radiant cooling ability, an optimal strategy is suggested to apply nighttime radiative cooling for D-AWH under high RH or boost the water sorption of sorbents for enhanced S-AWH if the nighttime RH is low. Importantly, daytime radiative cooling should be well employed to lower the water condensation temperature and increase the water collection of S-AWH, as the daytime RH is too low to activate D-AWH in arid regions. The synergistic utilization of radiative

cooling can enable the hybrid AWH to realize highly efficient water production.

## Conclusions

In summary, we have demonstrated a low-carbon sustainable strategy for realizing energy-efficient all-day AWH by synergistically harvesting heat from natural sunlight and coldness from the cold universe. An all-in-one hybrid AWH device with high water productivity, for the first time to our knowledge, is developed by integrating daytime radiative cooling-enhanced sorption-based AWH (S-AWH) and nighttime radiative cooling-driven dew-based AWH (D-AWH). To take full advantage of all-day radiative cooling for efficient AWH, transmittance-type radiative cooling (TRC) is introduced to the hybrid AWH device with layer-by-layer assembly to realize compact solar collection and radiative cooling at the same occupied physical area. The water productivity of S-AWH is improved by an enlarged temperature difference between water desorption and water condensation, ascribed to a lower condensation temperature by daytime radiative cooling. Together with the extra dew water collection at night by nighttime radiative cooling, the engineered all-in-one hybrid AWH device exhibits an impressive all-day water production of up to  $3654 \text{ g m}^{-2} \text{ day}^{-1}$ . Our approach provides a deep understanding of thermal design for next-generation highly efficient atmospheric water harvesting devices.

## Experimental methods

### Synthesis and water desorption tests of composite sorbent, LiCl@rGO-SA

LiCl@rGO-SA was prepared based on the directional freezing method, and detailed information about the synthesis can be found in our previous article.<sup>29</sup> A graphene oxide GO aqueous suspension was mixed with the sodium alginate (SA) solution, and deionized water in a weight ratio of 1:2:1. The mixture was poured into the molds (diameter, 10 cm). After directional ice crystal growth, the ice was removed in a vacuum dryer for three days. The porous matrix was then cross-linked by immersing it in  $\text{CaCl}_2$  solution. The cross-linked GO-SA porous matrix was subsequently treated at  $120 \text{ }^\circ\text{C}$  and thermally reduced to be rGO-SA. Finally, the LiCl@rGO-SA was obtained by soaking the rGO-SA matrix in LiCl solution and drying at  $90 \text{ }^\circ\text{C}$ . The water desorption test of sorbents was performed on a thermogravimetric analyzer (STA 449C from Netzsch), equipped with a moisture humidity generator (MHG 32 from ProUmid) under different water vapor pressures of 7.4 kPa, 4.2 kPa, and 2.3 kPa, corresponding to saturated vapor pressures at condensation temperatures of  $40 \text{ }^\circ\text{C}$ ,  $30 \text{ }^\circ\text{C}$ , and  $20 \text{ }^\circ\text{C}$ , respectively.

### Fabrication of the all-in-one hybrid atmospheric water harvesting device

The hybrid atmospheric water harvesting (AWH) device majorly consists of the following parts: the water sorbent sheet adhered

to the selective solar absorber ( $8.5 \text{ cm} \times 8.5 \text{ cm}$ ), the solar-transparent radiative cooler using a PDMS membrane ( $10 \text{ cm} \times 10 \text{ cm}$ ) coated on the PET membrane, the aluminum finned heat sinks, the thermal insulation panels between sorbent and radiative cooler, and the enclosures. The water sorbent sheet with a diameter of about 8 cm was adhered on the back side of a commercial selective solar absorber (provided by Linuo Paradigma Solar Company, Shan Dong, China) by using thermal conductive silica gel. Four aluminum finned heat sinks ( $106 \text{ mm} \times 25 \text{ mm}$  with fin height of 31 mm and fin spacing of 3.7 mm) were installed in the hybrid water harvester to cover part of the condensation heat. The thermal insulation panel is composed of two PE porous membranes for allowing mass transfer and reducing air convection. The PDMS-PET membrane was fixed by using several acrylic strips, covered by aluminum foils for reducing the solar absorbance of the surroundings. In addition to the PDMS-PET membrane, other materials can be explored to realize reliable transmittance-type radiative cooling such as transparent silica aerogel.<sup>57</sup> The materials of enclosures are acrylic panels, packed with thermal insulation cotton for reducing the heat losses during the solar collection process. The acrylic enclosures were assembled with aluminum finned heat sinks by glue. Above the PDMS-PET membrane, aluminum finned heat sinks, and enclosures are assembled and sealed by rubber rings, screws, and clips. For a comparative study, a similar device was fabricated using the same components except for replacing the PDMS-PET membrane with a PE membrane. To measure the temperatures of solar heating, thermal insulation panels, and PDMS-PET membrane, three k-type superfine thermocouples were installed at different locations. Two temperature and humidity sensors were used to measure the water vapor pressures near the sorbents at two devices and another one was put under a shadowing to measure the temperature and relative humidity of ambient air. The k-type thermocouples were calibrated by using a standard temperature calibration oil bath at different temperatures from 0 to  $100 \text{ }^\circ\text{C}$ . Two weighting sensors were installed to test the mass change of sorbents during the water release-condensation process in the daytime and the water sorption process at night. The two water harvesting devices were put in a plane with an inclined angle of  $30^\circ$  by considering the latitude of Shanghai ( $31^\circ \text{ N}$ ).

### Outdoor testing of the all-in-one AWH performance

The sorbents capture water at  $30 \text{ }^\circ\text{C}$ , 50% RH overnight in a constant temperature and humidity chamber before the outdoor tests. The outdoor comparison experiments of daytime S-AWH were carried out on May 1, 2021, and the continuous multiple S-AWH cycles during daytime were carried out on Aug. 4, 2022, both on the roof of our Green Energy Lab (GEL), located in the campus of Shanghai Jiao Tong University (SJTU), Shanghai, China. Arid-climates all-day AWH tests were conducted from Mar. 6, 2024, to Mar. 10, 2024, at Yunnan Normal University, Kunming, China. Before the testing, these two devices were covered with aluminum foil to reach the same starting temperatures. During the water collection process, an

IR camera was employed to measure the temperature changes of the PDMS-PET membrane, and a digital camera was used to record the water condensation process. A pyranometer was used to record the solar irradiation intensity. The real-time signals from these sensors were collected using a data collector (34970A, Agilent) and recorded on a computer. The outdoor experiments of nighttime D-AWH were carried out on May 1, Jun. 6, and Jun. 22, on the roof of our lab under different ambient conditions. The two devices were opened to let the ambient moisture diffuse in, where the mass change of sorbent was recorded by weighing sensors. Considering the weak influence of sorbent on the dew water condensation on PDMS-PET at night, the mass change of PDMS-PET was measured by putting the PDMS-PET on an electronic balance.

## Author contributions

T. L. and J. X. conceived and designed the experiment. J. X. and T. L. carried out the thermal design and energy analysis of the AWH device. J. X. and X. H. constructed and tested AWH devices. J. X. and T. L. wrote and revised the manuscript. All the authors discussed the results and commented on the manuscript. T. L. supervised the project.

## Conflicts of interest

There are no conflicts to declare.

## Acknowledgements

This work was supported by the National Natural Science Foundation of China for Young Scientists under contract No. 52206266, the National Natural Science Funds for Distinguished Young Scholar of China under contract No. 52325601, and the Major Program of National Natural Science Foundation of China under contract No. 52293412. This work was also supported by the China National Postdoctoral Program for Innovative Talents (BX20220202) and the General Project of China Postdoctoral Science Foundation (2022M712041). The authors would like to acknowledge Prof. Ming Li and Prof. Qiongfeng Yu for providing facilities and space for outdoor tests in Kunming.

## References

- J. Lord, A. Thomas, N. Treat, M. Forkin, R. Bain and P. Dulac, *et al.*, Global potential for harvesting drinking water from air using solar energy, *Nature*, 2021, **598**, 611–617.
- M. J. Kalmutzki, C. S. Diercks and O. M. Yaghi, Metal-organic frameworks for water harvesting from air, *Adv. Mater.*, 2018, **30**, 1704304.
- T. Oki and S. Kanae, Global hydrological cycles and world water resources, *Science*, 2006, **313**, 1068–1072.
- K. Yang, T. Pan, Q. Lei, X. Dong, Q. Cheng and Y. Han, A roadmap to sorption-based atmospheric water harvesting: from molecular sorption mechanism to sorbent design and system optimization, *Environ. Sci. Technol.*, 2021, **55**, 6542–6560.
- J. Xu, P. Wang, Z. Bai, H. Cheng, R. Wang, L. Qu and T. Li, Sustainable moisture energy, *Nat. Rev. Mater.*, 2024, DOI: [10.1038/s41578-023-00643-0](https://doi.org/10.1038/s41578-023-00643-0).
- Y. Tu, R. Wang, Y. Zhang and J. Wang, Progress and expectation of atmospheric water harvesting, *Joule*, 2018, **2**, 1452–1475.
- R. Li and P. Wang, Sorbents, processes and applications beyond water production in sorption-based atmospheric water harvesting, *Nat. Water*, 2023, **1**, 573–586.
- H. Kim, S. Yang, S. R. Rao, S. Narayanan, E. A. Kapustin, H. Furukawa, A. S. Umans, O. M. Yaghi and E. N. Wang, Water harvesting from air with metal-organic frameworks powered by natural sunlight, *Science*, 2017, **356**, 430–434.
- H. Kim, S. R. Rao, E. A. Kapustin, L. Zhao, S. Yang, O. M. Yaghi and E. N. Wang, Adsorption-based atmospheric water harvesting device for arid climates, *Nat. Commun.*, 2018, **9**, 1191.
- F. Fathieh, M. J. Kalmutzki, E. A. Kapustin, P. J. Waller, J. Yang and O. M. Yaghi, Practical water production from desert air, *Sci. Adv.*, 2018, **4**, eaat3198.
- W. Xu and O. M. Yaghi, Metal-organic frameworks for water harvesting from air, anywhere, anytime, *ACS Cent. Sci.*, 2020, **6**, 1348–1354.
- F. Ni, P. Xiao, C. Zhang and T. Chen, Hygroscopic polymer gels toward atmospheric moisture exploitations for energy management and freshwater generation, *Matter*, 2022, **5**, 2624–2658.
- F. Zhao, X. Zhou, Y. Liu, Y. Shi, Y. Dai and G. Yu, Super moisture-absorbent gels for all-weather atmospheric water harvesting, *Adv. Mater.*, 2019, **31**, 1806446.
- D. K. Nandakumar, Y. Zhang, S. K. Ravi, N. Guo, C. Zhang and S. C. Tan, Solar energy triggered clean water harvesting from humid air existing above sea surface enabled by a hydrogel with ultrahigh hygroscopicity, *Adv. Mater.*, 2019, **31**, 1806730.
- X. Zhou, P. Zhang, F. Zhao and G. Yu, Super moisture absorbent gels for sustainable agriculture via atmospheric water irrigation, *ACS Mater. Lett.*, 2020, **2**, 1419–1422.
- P. A. Kallenberger and M. Fröba, Water harvesting from air with a hygroscopic salt in a hydrogel-derived matrix, *Commun. Chem.*, 2018, **1**, 28.
- R. Li, Y. Shi, M. Alsaedi, M. Wu, L. Shi and P. Wang, Hybrid hydrogel with high water vapor harvesting capacity for deployable solar-driven atmospheric water generator, *Environ. Sci. Technol.*, 2018, **52**, 11367–11377.
- J. Yang, X. Zhang, H. Qu, Z. G. Yu, Y. Zhang, T. J. Eey, Y. Zhang and S. C. Tan, A Moisture-hungry copper complex harvesting air moisture for potable water and autonomous urban agriculture, *Adv. Mater.*, 2020, **32**, 2002936.
- J. Xu, T. Li, J. Chao, S. Wu, T. Yan, W. Li, B. Cao and R. Wang, Efficient solar-driven water harvesting from arid air with metal-organic frameworks modified by hygroscopic salt, *Angew. Chem., Int. Ed.*, 2020, **59**, 5202–5210.

- 20 T. Li, T. Yan, P. Wang, J. Xu, X. Huo and Z. Bai, *et al.*, Scalable and efficient solar-driven atmospheric water harvesting enabled by bidirectionally aligned and hierarchically structured nanocomposites, *Nat. Water*, 2023, **1**, 971–981.
- 21 A. Terzis, A. Ramachandran, K. Wang, M. Asheghi, K. E. Goodson and J. G. Santiago, High-frequency water vapor sorption cycling using fluidization of metal-organic frameworks, *Cell Rep. Phys. Sci.*, 2020, **1**, 100057.
- 22 A. LaPotin, Y. Zhong, L. Zhang, L. Zhao, A. Leroy, H. Kim, S. Rao and E. N. Wang, Dual-stage atmospheric water harvesting device for scalable solar-driven water production, *Joule*, 2021, **5**, 166–182.
- 23 N. Hanikel, M. S. Prévot, F. Fathieh, E. A. Kapustin, H. Lyu, H. Wang, N. J. Diercks, T. G. Glover and O. M. Yaghi, Rapid cycling and exceptional yield in a metal-organic framework water harvester, *ACS Cent. Sci.*, 2019, **5**, 1699–1706.
- 24 R. Li, Y. Shi, M. Wu, S. Hong and P. Wang, Improving atmospheric water production yield: Enabling multiple water harvesting cycles with nano sorbent, *Nano Energy*, 2020, **67**, 104255.
- 25 J. Y. Wang, R. Z. Wang, Y. D. Tu and L. W. Wang, Universal scalable sorption-based atmosphere water harvesting, *Energy*, 2018, **165**, 387–395.
- 26 L. Hua, J. Xu and R. Wang, Exergy-efficient boundary and design guidelines for atmospheric water harvesters with nano-porous sorbents, *Nano Energy*, 2021, **85**, 105977.
- 27 N. Hanikel, D. Kurandina, S. Chheda, Z. Zheng, Z. Rong, S. E. Neumann, J. Joachim Sauer, J. I. Siepmann, L. Gagliardi and O. M. Yaghi, MOF linker extension strategy for enhanced atmospheric water harvesting, *ACS Cent. Sci.*, 2023, **9**, 551–557.
- 28 W. Song, Z. Zheng, A. H. Alawadhi and O. M. Yaghi, MOF water harvester produces water from Death Valley desert air in ambient sunlight, *Nat. Water*, 2023, **1**, 626–634.
- 29 J. Xu, T. Li, T. Yan, S. Wu, M. Wu, J. Chao, X. Huo, P. Wang and R. Wang, Ultrahigh solar-driven atmospheric water production enabled by scalable rapid-cycling water harvester with vertically aligned nanocomposite sorbent, *Energy Environ. Sci.*, 2021, **14**, 5979–5994.
- 30 G. Ni, G. Li, S. V. Boriskina, H. Li, W. Yang, T. Zhang and G. Chen, Steam generation under one sun enabled by a floating structure with thermal concentration, *Nat. Energy*, 2016, **1**, 16126.
- 31 J. Mandal, Y. Yang, N. Yu and A. P. Raman, Paints as a scalable and effective radiative cooling technology for buildings, *Joule*, 2020, **4**, 1350–1356.
- 32 W. Li, M. Dong, L. Fan, J. J. John, Z. Chen and S. Fan, Nighttime radiative cooling for water harvesting from solar panels, *ACS Photonics*, 2020, **8**, 269–275.
- 33 W. J. Hamilton and M. K. Seely, Fog basking by the Namib Desert beetle, *Onymacris unguicularis*, *Nature*, 1976, **262**, 284–285.
- 34 M. Zhou, H. Song, X. Xu, A. Shahsafi, Y. Qu, Z. Xia, Z. Ma, M. A. Kats, J. Zhu, B. S. Ooi, Q. Gan and Z. Yu, Vapor condensation with daytime radiative cooling. *Proc. Natl. Acad. Sci.*, 2021, **118**, e2019292118.
- 35 I. Haechler, H. Park, G. Schnoering, T. Gulich, M. Rohner, A. Tripathy, A. Milionis, T. M. Schutzius and D. Poulikakos, Exploiting radiative cooling for uninterrupted 24-hour water harvesting from the atmosphere, *Sci. Adv.*, 2021, **7**, eabf3978.
- 36 Y. Wang, S. Gao, H. Zhong, B. Zhang, M. Cui, M. Jiang, S. Wang and Z. Wang, Heterogeneous wettability and radiative cooling for efficient deliquescent sorbents-based atmospheric water harvesting, *Cell Rep. Phys. Sci.*, 2022, **3**, 100879.
- 37 W. Zhu, Y. Zhang, C. Zhang, X. Shan, A. K. Rao and S. L. Pitts, *et al.*, Radiative cooling sorbent towards all weather ambient water harvesting, *Commun. Eng.*, 2023, **2**, 35.
- 38 Y. Zhang, W. Zhu, C. Zhang, J. Peoples, X. Li, A. L. Felicelli, X. Shan, D. M. Warsinger, T. Borca-Tasciuc, X. Ruan and T. Li, Atmospheric water harvesting by large-scale radiative cooling cellulose-based fabric, *Nano Lett.*, 2022, **22**, 2618–2626.
- 39 T. Li, M. Wu, J. Xu, R. Du, T. Yan and P. Wang, *et al.*, Simultaneous atmospheric water production and 24-hour power generation enabled by moisture-induced energy harvesting, *Nat. Commun.*, 2022, **13**, 6771.
- 40 H. L. Nguyen, N. Hanikel, S. J. Lyle, C. Zhu, D. M. Proserpio and O. M. Yaghi, A porous covalent organic framework with voided square grid topology for atmospheric water harvesting, *J. Am. Chem. Soc.*, 2020, **142**, 2218–2221.
- 41 J. Remund, S. Müller, M. Schmutz and P. Graf, Meteoronorm version 8. METEOTEST, <https://www.meteotest.com> (accessed January 2022).
- 42 J. L. Kou, Z. Jurado, Z. Chen, S. Fan and A. J. Minnich, Daytime radiative cooling using near-black infrared emitters, *ACS Photonics*, 2017, **4**, 626–630.
- 43 O. A. Alduchov and R. E. Eskridge, Improved Magnus form approximation of saturation vapor pressure, *J. Appl. Meteorol. Climatol.*, 1996, **35**, 601–609.
- 44 W. Guan, C. Lei, Y. Guo, W. Shi and G. Yu, Hygroscopic-microgels-enabled rapid water extraction from arid air, *Adv. Mater.*, 2023, **35**, e2300296.
- 45 L. Garzón-Tovar, J. Pérez-Carvajal, I. Imaz and D. Maspoch, Composite salt in porous metal-organic frameworks for adsorption heat transformation, *Adv. Funct. Mater.*, 2017, **27**, 1606424.
- 46 H. An, Y. Chen, Y. Wang, X. Liu, Y. Ren and Z. Kang, *et al.*, High-performance solar-driven water harvesting from air with a cheap and scalable hygroscopic salt modified metal-organic framework, *Chem. Eng. J.*, 2023, **461**, 141955.
- 47 T. Yan, T. Li, J. Xu, J. Chao, R. Wang and Y. I. Aristov, *et al.*, Ultrahigh-energy-density sorption thermal battery enabled by graphene aerogel-based composite sorbents for thermal energy harvesting from air, *ACS Energy Lett.*, 2021, **6**, 1795–1802.
- 48 F. B. Cortés, F. Chejne, F. Carrasco-Marín, C. Moreno-Castilla and A. F. Pérez-Cadenas, Water adsorption on zeolite 13X: comparison of the two methods based on mass

- spectrometry and thermogravimetry, *Adsorption*, 2010, **16**, 141–146.
- 49 R. H. Mohammed, O. Mesalhy, M. L. Elsayed, M. Su and L. C. Chow, Revisiting the adsorption equilibrium equations of silica-ge/water for adsorption cooling applications, *Int. J. Refrig.*, 2018, **86**, 40–47.
- 50 M. V. Solovyeva, L. G. Gordeeva, T. A. Krieger and Y. I. Aristov, MOF-801 as a promising material for adsorption cooling: Equilibrium and dynamics of water adsorption, *Energy Convers. Manage.*, 2018, **174**, 356–363.
- 51 A. J. Rieth, S. Yang, E. N. Wang and M. Dincă, Record atmospheric fresh water capture and heat transfer with a material operating at the water uptake reversibility limit, *ACS Cent. Sci.*, 2017, **3**, 668–672.
- 52 N. Hanikel, X. Pei, S. Chheda, H. Lyu, W. Jeong, J. Sauer, L. Gagliardi and O. M. Yaghi, Evolution of water structures in metal-organic frameworks for improved atmospheric water harvesting, *Science*, 2021, **374**, 454–459.
- 53 H. Qi, T. Wei, W. Zhao, B. Zhu, G. Liu, P. Wang, Z. Lin, X. Wang, X. Li, X. Zhang and J. Zhu, An interfacial solar-driven atmospheric water generator based on a liquid sorbent with simultaneous adsorption–desorption, *Adv. Mater.*, 2019, **31**, 1903378.
- 54 J. Y. Wang, J. Y. Liu, R. Z. Wang and L. W. Wang, Experimental investigation on two solar-driven sorption based devices to extract fresh water from atmosphere, *Appl. Therm. Eng.*, 2017, **127**, 1608–1616.
- 55 H. Shan, C. Li, Z. Chen, W. Ying, P. Poredoš, Z. Ye, Q. Pan, J. Wang and R. Wang, Exceptional water production yield enabled by batch-processed portable water harvester in semi-arid climate, *Nat. Commun.*, 2022, **13**, 5406.
- 56 J. D. Kocher and A. K. Menon, Addressing global water stress using desalination and atmospheric water harvesting: a thermodynamic and technoeconomic perspective, *Energy Environ. Sci.*, 2023, **16**, 4983–4993.
- 57 L. Zhao, B. Bhatia, S. Yang, E. Strobach, L. A. Weinstein, T. A. Cooper, G. Chen and E. N. Wang, Harnessing heat beyond 200 °C from unconcentrated sunlight with nonevacuated transparent aerogels, *ACS Nano*, 2019, **13**, 7508–7516.